Research Article

Yusaku Seimiya*, Shuto Tomita, Tohei Kawaguchi, Hidekazu Kobatake, Jürgen Brillo, Suguru Shiratori, Ken-ichi Sugioka, Takehiko Ishikawa, and Shumpei Ozawa

Round-robin measurement of surface tension of high-temperature liquid platinum free of oxygen adsorption by oscillating droplet method using levitation techniques

https://doi.org/10.1515/htmp-2022-0306
received October 27, 2023; accepted December 14, 2023

Abstract: Round-robin measurement of surface tension of high-temperature liquid platinum was conducted free of any contamination from the supporting materials and oxygen adsorption, using an electrostatic levitator (ESL), two electromagnetic levitator (EML), and an aerodynamic levitator (ADL). The measured temperature dependences of the surface tension using ESL and two EMLs were in good agreement and were expressed as $\sigma = 1{,}798 \pm 74.3 - (0.12 \pm 0.0445) \times (T - 2{,}041)$ [10^{-3} N·m^{-1}] (1,900–2,600 K). However, the surface tension values measured with ADL were slightly lower than those exceeding the uncertainty of the measurement plots at high temperatures.

Keyword: High temperature melt, thermophysical properties, electrostatic levitation, electromagnetic levitation, aerodynamics levitation

*** Corresponding author: Yusaku Seimiya,** Department of Advanced Materials Science and Engineering, Chiba Institute of Technology, Narashino 275-0016, Japan, e-mail: s1521193DL@s.chibakoudai.jp
Shuto Tomita, Tohei Kawaguchi, Shumpei Ozawa: Department of Advanced Materials Science and Engineering, Chiba Institute of Technology, Narashino 275-0016, Japan
Hidekazu Kobatake: Organization for Research Initiatives & Development, Doshisha University, Kyotanabe 610-0394, Japan
Jürgen Brillo: Institute of Materials Physics in Space, German Aerospace Center (DLR), 51147 Cologne, Germany
Suguru Shiratori: Department of Mechanical Systems Engineering, Tokyo City University, Tokyo 1-28-1, Japan
Ken-ichi Sugioka: Department of Mechanical Systems Engineering, Toyama Prefectural University, Imizu 939-0398, Japan
Takehiko Ishikawa: Institute of Space and Astronautical Science, Japan Aerospace Exploration Agency (JAXA), Tsukuba 305-8505 Japan; SOKENDAI (The Graduate University for Advanced Studies), Sagamihara 252-5210, Japan
ORCID: Yusaku Seimiya 0000-0002-8448-6161; Hidekazu Kobatake 0000-0002-5054-6242; Jürgen Brillo 0000-0003-3712-0666; Suguru Shiratori 0000-0003-0158-6798; Ken-ichi Sugioka 0000-0002-8043-0590; Takehiko Ishikawa 0000-0001-8569-2074; Shumpei Ozawa 0000-0002-9674-1123

1 Introduction

Highly reliable data on the surface tension and its temperature dependence for high-temperature metallic melts are essential for the improvement and optimization of various high-temperature melt processes involving a free surface such as welding, brazing, and thermal spraying. To measure the surface tension of high-temperature melts, container-free measurements with the oscillating droplet method using levitation techniques such as electrostatic levitation (ESL) [1–5], electromagnetic levitation (EML) [5–14], and aerodynamic levitation (ADL) [15–18] have been increasingly employed to prevent sample contamination caused by supporting materials at high temperatures. The surface tension of a levitated droplet can be calculated using the following Rayleigh equation [19–23]:

$$\sigma = \frac{3}{8}\pi M f_{\mathrm{R}}^2, \tag{1}$$

where σ is the surface tension, M is the sample mass, and f_{R} is the frequency of surface oscillation for the $l = 2$ mode, called the Rayleigh frequency. However, the reported data for the surface tension of liquid metals such as titanium [5] and silicon [11] obtained using levitation techniques often show considerable scatter. This scatter is often attributed to the effects of sample purity and oxygen adsorption from the atmospheric gas without sufficient discussion. It is also possible that inherent errors associated with the measurement method and apparatus affect the results. To ensure the validity of the container-free measurements of surface tension of high-temperature metallic melts using ESL, EML, and ADL, and to guarantee the reliability of the results,

Open Access. © 2023 the author(s), published by De Gruyter. This work is licensed under the Creative Commons Attribution 4.0 International License.

conducting a round-robin test is indispensable, especially considering the effects of oxygen partial pressure in the measurement atmosphere.

In this study, we measured the surface tension of liquid platinum using container-free methods with ESL, two different EMLs, and ADL. Liquid platinum is highly chemically stable such that its surface tension is unaffected by oxygen adsorption, even when the measurements are conducted in open air. This study aimed to validate the container-free measurement of surface tension of a high-temperature melt using the three different aforementioned levitation techniques based on the results of round-robin tests. In addition, by using ESL, we measured the density of the liquid platinum required for the surface tension measurement.

2 Experimental procedure

2.1 ESL

The nomenclature used in this study is given in Table 1. Figure 1 shows a schematic diagram of the ESL used in this study, which is installed at the Japan Aerospace Exploration Agency (JAXA). A cubic platinum sample with a purity of 99.95 mass% and a mass of approximately 40 mg was placed between a pair of disk electrodes in a vacuum chamber. After the chamber was evacuated to the order of 10^{-5} Pa using a turbomolecular pump backed up by a

Table 1: Nomenclature

Symbol	Description
σ	Surface tension [N m^{-1}]
T	Temperature [K]
ρ	Density [kg m^{-3}]
r	Radius of the droplet [m]
Q	Sample charge [c]
E	Electric field applied to levitate the sample [V m^{-1}]
F	Correction term for the effects of charge and gravity on the frequency
M	Sample mass [kg]
G	Gravitational acceleration [m s^{-2}]
U	Potential difference between the top and bottom electrodes [V]
L	Distance between top and bottom electrodes [m]
ε_0	Permittivity of vacuum [F m^{-1}]
σ_0	Surface tension calculated without considering the correction term F
$R(\theta)$	Length from the center of gravity to the edge for the droplet [m]
θ	Polar angle [rad]
V	Volume [m^3]
f_R	Rayleigh frequency
l	Oscillation mode
m	Oscillation index
$f_{2,m}$	Frequencies of l = 2 mode (m = 0, ±1, and ±2) [Hz]
$f_{1,m}$	Frequencies of l = 1 for levitated droplet (m = 0 and ±1) [Hz]
ft	Frequency of translation oscillation [Hz]
A	Projected area of the top-view image of the levitated droplet
Rx	Radius of the droplet along the x−axis
Ry	Radius of the droplet along the y-axis
$f_{2,0}$	Frequency of surface oscillation m = 0 in l = 2 mode, [Hz]
$f_{2,\pm1}$	Frequency of surface oscillation m = ±1 in l = 2 mode, [Hz]
$f_{2,\pm2}$	Frequency of surface oscillation m = ±2 in l = 2 mode, [Hz]
$u(i)$	Standard uncertainty of each source
$c(i)$	Sensitivity coefficient of each source
$u_\rho(i)$	Uncertainty contributions of density measurement
$u_\sigma(i)$	Uncertainty contributions of surface-tension measurement
$d_{\mathrm{cal}}^{\mathrm{ref}}$	Calibration of micrometer
$d_{\mathrm{res}}^{\mathrm{ref}}$	Resolution of micrometer
$d_{\mathrm{rep}}^{\mathrm{ref}}$	Repeatability of diameter measurement for reference sphere
$dp_{\mathrm{res}}^{\mathrm{ref}}$	Resolution of image for reference sphere
$dp_{\mathrm{rep}}^{\mathrm{ref}}$	Repeatability of contour fitting for reference sphere
rp_{res}	Resolution of image for levitated droplet
rp_{rep}	Repeatability of contour fitting for levitated droplet
m_{cal}	Resolution of the electronic balances
m_{res}	Calibration of electronic balances
m_{rep}	Repeatability of mass measurement
f_{res}	Frequency resolution of FFT analysis
f_{rep}	Repeatability of identifying frequency peaks using FFT spectrum
L_{res}	Resolution of scale
L_{rep}	Repeatability of interelectrode distance measurement
U_{res}	Resolution of electrode potential control
U_{sta}	Stability of electrode potential control
$u_c(\rho)$	Combined standard uncertainty in the density measurement
$u_c(\sigma_{\mathrm{ESL}})$	Combined standard uncertainty in the surface-tension measurement using ESL
$u_c(\sigma_{\mathrm{EML}})$	Combined standard uncertainty in the surface-tension measurement using EML
$u_c(\sigma_{\mathrm{ADL}})$	Combined standard uncertainty in the surface-tension measurement using ADL
k_p	Coverage factor
u_{exp}	Expanded uncertainty
$\hat{\beta}$	Temperature coefficient
$\bar{\rho}$	Mean value of measured density
$\bar{T}$	Mean value of temperature
$\hat{\delta}_e$	Residual variance of measured data

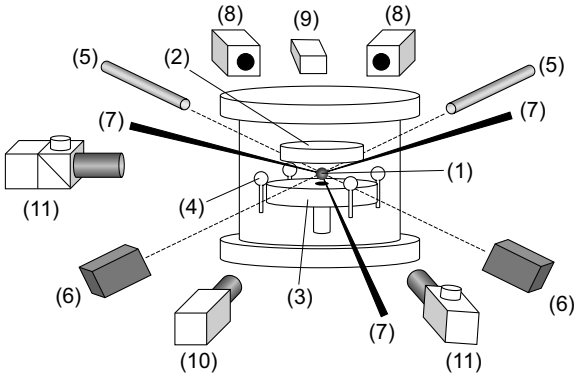

Figure 1: Schematic view of the ESL furnace and its diagnostic apparatus [3]: (1) sample, (2) top electrode, (3) bottom electrode, (4) side electrodes, (5) He–Ne lasers, (6) position detectors, (7) CO_2 laser beams, (8) pyrometers, (9) ultraviolet light, (10) CCD camera, (11) CCD cameras with telephoto objective lens.

scroll pump, the positively charged sample was electrostatically levitated by applying a high voltage between the electrodes. The levitated sample was heated and then melted by irradiation with 100 W CO_2 lasers from three directions [2]. The rotation of the levitated sample was controlled by appropriately aligning the CO_2 laser beams or by a rotating magnetic field generated by the four coils beneath the bottom electrode. The sample temperature was measured by monochromatic pyrometers. The emissivity setting of the pyrometers was adjusted so that the plateau temperature of the liquid phase after the recalescence at the cooling stage indicates the equilibrium melting point of platinum based on the valid assumption that the emissivity of the sample does not change with the temperature within the operating wavelength range.

A small sinusoidal electric field was superimposed on the levitation field to excite the surface oscillation of $m = 0$ for the $l = 2$ mode in the levitated droplet while monitoring the oscillation using an oscillation detection system composed of a power meter with a vertical slit at the sampling frequency of 4,096 Hz. The measured signal was analyzed using the fast Fourier transform (FFT) to determine the frequency of the $m = 0$ oscillation ($f_{2,0}$). The surface tension of liquid platinum, σ, was calculated from the frequency of the $m = 0$ oscillation using the following Rayleigh equation [19] modified for a nonuniform surface charge distribution [25,26]:

$$\sigma = \frac{r^3\rho}{8}\left\{(2\pi f_{2,0})^2 - \frac{Q^2}{8\pi^2 r^6 \rho\varepsilon_0}\right\}(1 - F(\sigma_0, q, e)), \quad (2)$$

where r is the radius of the droplet when it assumed a spherical shape, ρ is the density of liquid platinum, and ε_0 is the vacuum permittivity. Q is the droplet charge that is given by the following equation:

$$M{\cdot}G = \frac{QU}{L}, \quad (3)$$

where G is the gravitational acceleration, U is the potential difference between the top and bottom electrodes, and L is the spacing between the electrodes. $F(\sigma_0, q, e)$ is the correction term for the effect of the droplet deformation on $f_{2,0}$, which is defined as follows:

$$F(\sigma_0, q, e) = \frac{(243.31\sigma_0^2 - 63.14q^2\sigma_0 + 1.54q^4)E^2 r\varepsilon_0}{176\sigma_0^3 - 120q^2\sigma_0^2 + 27\sigma_0 q^4 - 2q^6}, \quad (4)$$

where σ_0 is the surface tension calculated without considering the correction term F. q and e are defined as follows:

$$q^2 = \frac{Q^2}{16\pi^2 r^3 \varepsilon_0}, \quad (5)$$

$$e^2 = \left(\frac{U}{L}\right)^2 r\varepsilon_0. \quad (6)$$

Since the electrostatically levitated droplet is axisymmetric along the vertical axis, its volume can be evaluated from the fitted data of the side view images of the droplet free of surface oscillation observed by three high-speed video (HSV) cameras in conjunction with the temperature, while cooling the sample according to the following equation:

$$V = \frac{2\pi}{3}\int_0^\pi R(\theta)^3 \sin\theta \mathrm{d}\theta, \quad (7)$$

where $R(\theta)$ is the length from the center of gravity to the edge for the droplet and θ is the polar angle. The density of liquid platinum for each temperature was determined from the sample mass M divided by the volume V.

$$\rho = \frac{M}{V}. \quad (8)$$

A more detailed description of the procedures for the surface tension and density measurements can be found in the previous studies [3,24].

2.2 EML

Two EMLs installed at the Chiba Institute of Technology (CIT) and the German Aerospace Center (DLR), respectively, were used to compare the results. The schematics of these facilities are shown in Figure 2. The major differences between these EML facilities are the shape and size of the EML coil and the frequency of high-frequency AC power; these differences usually affect the size of the metallic sample that can be levitated, the deformation of the levitated droplet, and the droplet rotation, as well as the ability to heat the sample. As a result, the frequencies

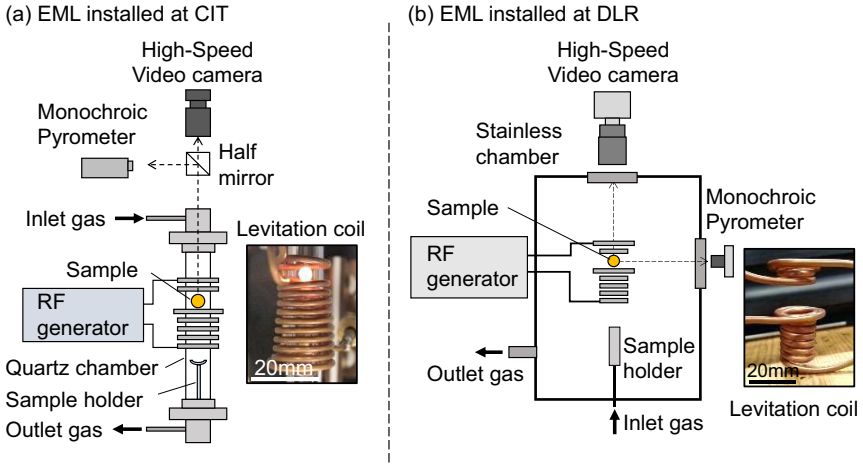

Figure 2: Schematic view of the EML furnace installed at (a) CIT and (b) DLR, and its diagnostic apparatus [7,8].

of the surface oscillations and translational oscillations of the levitated droplet, which are necessary to calculate the surface tension, are altered. Moreover, both the shape and size of the chamber differ for these EML facilities, which can affect the amount of oxygen adsorption from the measurement atmosphere on the levitated droplet that acts to decrease the surface tension.

A piece of the platinum sample with a mass of 1,600–3,000 mg was placed on a sample holder and was positioned in the center of the EML coil. The sample was first electromagnetically levitated and then melted under the flow of high-purity commercial helium gas. The temperature of the droplet was controlled by varying the flow rate of the helium gas using a monochromatic pyrometer. The emissivity setting of the pyrometer was adjusted so that the plateau temperature of the liquid phase during the melting of the sample was equal to the equilibrium melting point of platinum. After the droplet temperature became constant, the oscillation of the droplet was monitored from above using a HSV camera at 500 fps for 16.4 s at CIT and at 800 fps 6.4 s at DLR.

The frequencies of the surface oscillations of m = 0, ±1, and ±2 for the l = 2 mode and those of the center of gravity (oscillations of the m = 0 and ±1 for the l = 1 mode) were obtained from time-sequence data of the HSV images using FFT analysis. The frequencies of the m = 0, ±1, and ±2 oscillations can be identified based on the rule shown in Table 2, where A is the area of the projection image of the levitated droplet, R^+ is the sum of the radii along the x and y axes, R_x and R_y, and R^- is the difference between R_x and R_y [22,23]. The influence of the apparent droplet rotations, induced by the phase differences between m = +1 and m = –1, and m = +2 and m = –2, was considered, of real rotation in the analysis [23]. The surface tension of liquid platinum was calculated from

Table 2: Relationship among oscillation of m = 0, ±1, and ±2, corresponding to that of area, A, R_x, and R_y

	m = 0	m = ±1	m = ±2
A	Yes	Yes	No
$R_x + R_y$	Yes	Yes	No
$R_x - R_y$	No	Yes	Yes

these frequencies using the following Rayleigh equation [19], calibrated with the Cummings and Blackburn equation [27]:

$$\sigma = \frac{3}{8}\pi M\left[\frac{1}{5}\sum_{m=-2}^{2} f_{2,m}^2 - f_t^2\left\{1.905 + 1.200 \times \left(\frac{G}{8\pi^2 f_t^2}\sqrt[-3]{\frac{3M}{4\pi\rho}}\right)^2\right\}\right], \tag{9}$$

$$f_t = \frac{1}{3}\sum_{m=-1}^{1} f_{1,m}, \tag{10}$$

where $f_{2,m}$ are the frequencies of surface oscillation for m = 0, ±1, and ±2 for the l = 2 mode, and f_t are the frequencies of the motion of the center of gravity of the droplet. Detailed descriptions of the measurement procedures and facilities can be found elsewhere [7,8].

2.3 ADL

A small cube of platinum (40 mg) was rapidly melted on a p-BN plate in the air by irradiation with a semiconductor laser beam and was then immediately solidified into a spherical shape with a diameter of 1.6 mm. The spherical

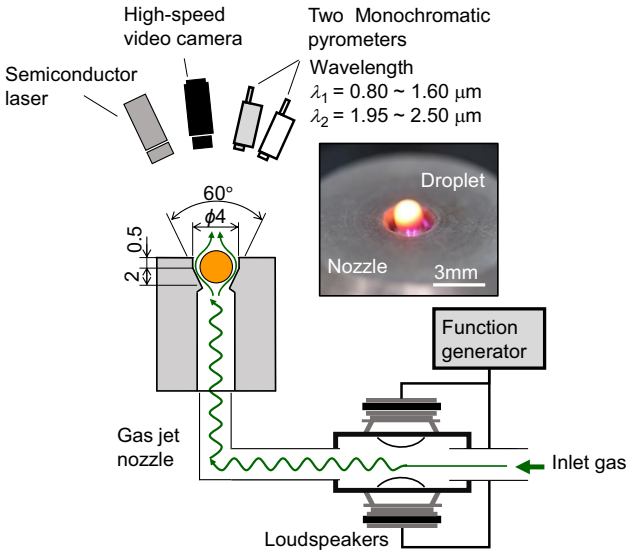

Figure 3: Schematic view of the ADL furnace.

sample was placed on a nozzle of the ADL, as schematically shown in Figure 3, and then levitated on an argon gas jet from the bottom at a rate of approximately 0.9 L·min^{-1} controlled by a digital mass flow controller. The levitated sample was heated and melted by irradiation with the semiconductor laser. The temperature of the levitated droplets was controlled by varying the laser output while simultaneously using two monochromatic pyrometers with different wavelengths, λ_1 = 0.8–1.6 μm and λ_2 = 1.95–2.5 μm, where the emissivity settings of the pyrometers were adjusted to obtain the same temperature under the assumption that the sample is a gray body [28]. When the droplet temperature became constant, a sound wave was applied to the gas jet prior to its introduction into the ADL nozzle using two loudspeakers facing each other so that surface oscillation of m = 0 for the l = 2 mode is excited in the levitated droplet. After turning off the sound wave applied to the gas jet, the behavior of the surface oscillations of the droplet was monitored with an HSV camera at 2,000 fps for less than 1 s until the surface oscillation of the droplet was damped.

The frequency of the surface oscillation of m = 0 for the l = 2 mode was determined from time-sequence data of the droplet diameter using the FFT. The surface tension of liquid platinum was calculated from the frequency of the surface oscillation of m = 0 for the l = 2 mode and the sample mass after the experiment using the Rayleigh equation (equation (1)) [15,16,19].

3 Results

Figure 4 shows the density of liquid platinum as a function of temperature, T, measured with ESL, along with the literature data presented for comparison [4,29–34]. The density of liquid platinum was measured over a wide temperature range of approximately 500 K between 1,700–2,200 K, including the undercooling region. Since the measured density decreases linearly with the increasing temperature, it can be described by a linear approximation based on the plotted measurement results as follows:

$$\rho = 18{,}906 - 1.0852(T - 2{,}041)[\mathrm{kg{\cdot}m^{-3}}], \qquad (11)$$

which is in relatively good agreement with the results reported by Gather et al. [31] and Ishikawa et al. [4].

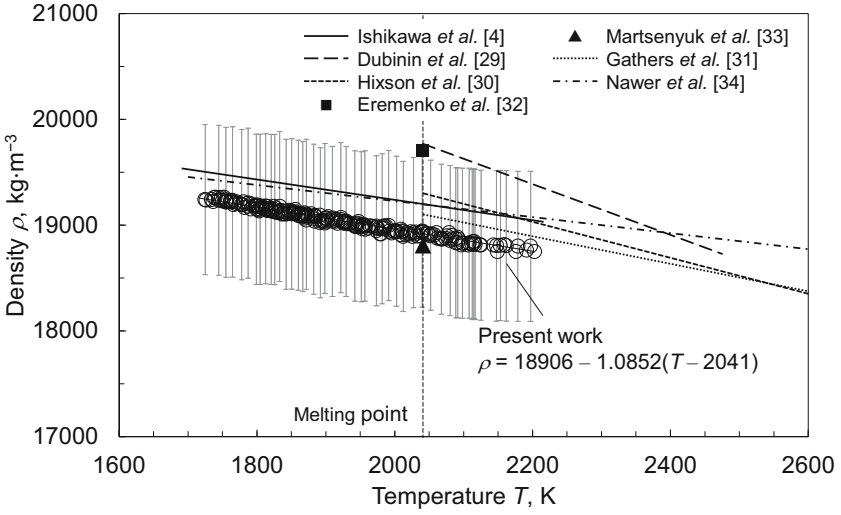

Figure 4: Density of liquid platinum measured using the ESL method together with the literature data [4,29–34].

Figure 5 shows a typical frequency spectrum for the surface oscillation of the droplet levitated by the ESL, as obtained by the FFT analysis. Only one distinct peak appears in the spectrum, indicating that only the m = 0 oscillation for the l = 2 mode is excited in the droplet by ESL.

Figure 6 shows typical frequency spectra of oscillations of A, R^+, and R^- for the droplets levitated by the EMLs installed at CIT (Figure 6(a)) and DLR (Figure 6(b)). In the EML technique, the single surface oscillation of the l = 2 mode, known as the Rayleigh oscillation, splits into three, corresponding to oscillations of m = 0, ±1, and ±2 because of the droplet deformation due to the gravitational acceleration and the electromagnetic forces from the levitation coil [27]. Furthermore, the frequency peaks of the surface oscillations for m = ±1 and ±2 are symmetrically split into two when the droplet rotates around an axis perpendicular to the projection plane, as is usually observed in an electromagnetically levitated droplet, even though the frequencies of the surface oscillations are actually unchanged. As a result, five peaks are usually observed in the frequency spectra of oscillations of the A, R^+, and R^- for the droplet levitated by EML, as shown in the spectra obtained in the experiments carried out at CIT and DLR. Since the surface oscillation in the levitated droplet was observed for a slightly longer time in the experiment carried out at CIT (16.4 s) than in the experiment carried out at DLR (6.5 s), the FFT spectra presented in Figure 6(a) that were obtained in the former experiment appear to be somewhat noisy due to the higher resolution. The discrepancies in the frequencies of the surface oscillations for m = 0, ±1, and ±2 between the spectra presented in Figure 6(a) and (b) stem from differences in the droplet size as well as the temperature.

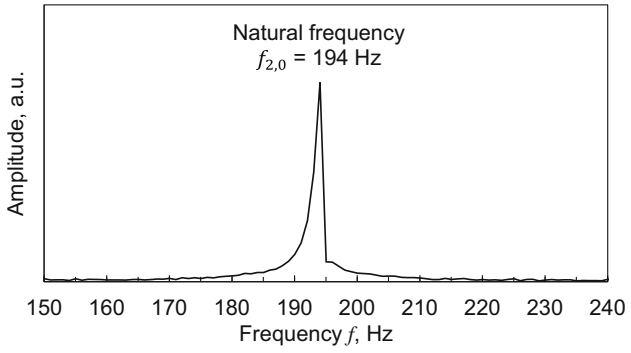

Figure 5: FFT results of a typical oscillation signal obtained from a liquid platinum levitated by ESL.

Figure 7 shows the typical examples of the frequency spectra of the oscillation of the droplet diameter in ADL. These were obtained from the experiments in which the surface oscillation of the droplet was repeatedly excited and damped by turning the sound waves of different frequencies applied to the gas jet on and off while the droplet was levitated and maintained at 2,500 K. When the frequency of the sound wave applied to the gas jet is varied from 180 to 210 Hz, the spectra consistently show a peak at approximately 191 Hz along with a peak corresponding to the frequency of the sound wave for all of the sound wave frequencies. When the frequency of the applied sound wave is far from 191 Hz, only a single peak corresponding to the sound wave frequency was detected in the spectra. These results indicate that the peak at 191 Hz corresponds

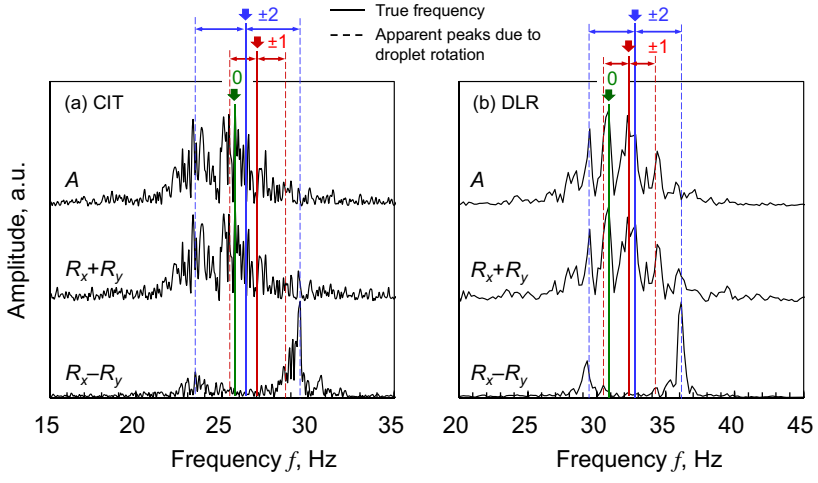

Figure 6: Surface oscillation frequency peaks of m = 0, ±1, ±2 obtained from the results of the FFT analysis of the oscillation behavior of liquid platinum levitated by the EML installed at (a) CIT and (b) DLR. The frequencies of m = ±1 and ±2 split into two peaks due to droplet rotation.

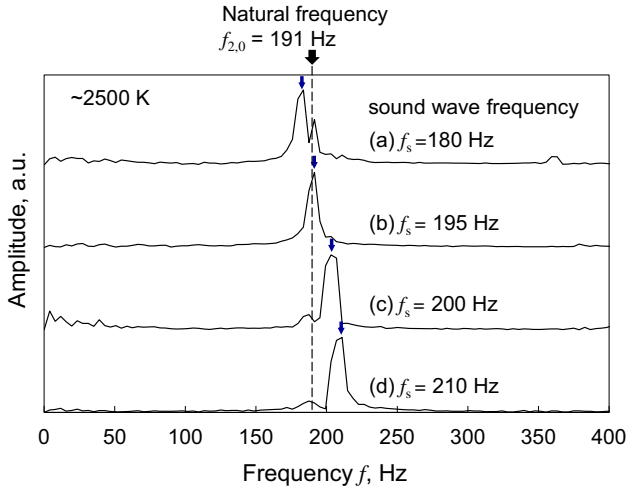

Figure 7: Two peaks were obtained from the FFT analysis of the surface oscillation behavior when the oscillation was excited by applying sound waves to the liquid platinum levitated by the ADL. The first peak shifted from 180 to 210 Hz according to the sound wave frequency. The frequency of the second peak was constant at 191 Hz, indicating that this was the natural frequency.

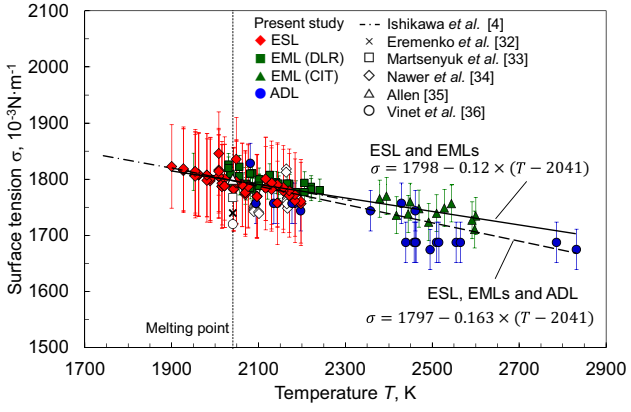

Figure 8: Comparison of the measurement results of the surface tension of liquid platinum by ESL (◆), EML (DLR: ■, CIT: ▲), and ADL (●) together with the literature data [4,32–36].

to the natural frequency of the surface oscillation of the levitated droplet.

Figure 8 displays the temperature dependence of the surface tension of liquid platinum as measured using ESL, two EMLs, and ADL together with literature data [4,32–36] for comparison. Uncertainty bars for each plot were evaluated on the basis of the ISO Guide to the Expression of Uncertainty in Measurement (GUM) [37], with a selected coverage factor of k_p = 2. The evaluation of these uncertainties is described in detail in the next section. Table 3 presents a summary of the measurement results obtained with these four apparatuses. The surface tension of liquid platinum measured using ESL (◆) decreases linearly with the increasing temperature, which is in good agreement with the data reported by Ishikawa et al. [4] and Allen [35].

Although the measured temperature ranges show a significant discrepancy between the measurements using two different EMLs (▲, ■) due to their different coil shapes, the temperature dependence of the surface tension revealed in these measurements agrees well with the results obtained using ESL, as indicated by the solid line. This suggests the validity of the measurement methods for the surface tension of high-temperature metallic melt using ESL and EML. Consequently, the temperature dependence of the surface tension of liquid platinum can be expressed using a linear least-squares method based on the measurement data obtained using ESL and EMLs as follows:

$$\sigma = 1{,}798 - 0.12(T - 2{,}041) \quad [10^{-3}\mathrm{N{\cdot}m^{-1}}]. \tag{12}$$

The intercept of 1,798 × 10^{-3} N·m^{-1} corresponds to the surface tension at the melting temperature of platinum (2,041 K).

Conversely, the surface tension values of liquid platinum measured using ADL (●) appear to be lower than the values measured with ESL and EMLs throughout the entire measurement temperature range. As a result, when using the least-squares method to calculate the temperature dependence of the surface tension based on all of the plots of measurement results obtained with ESL, two EMLs, and ADL, the surface tension gradient with respect to temperature becomes steeper as indicated by the dotted line. Notably, many of the plots of the data obtained at high temperatures with EML and ADL measurements deviate from this approximation line, confirming the deviation of the measurement results with ADL from those with ESL and EMLs.

Table 3: Results of a round robin measurement of the surface tension of liquid platinum using the droplet oscillation method with ESL, EML, and ADL

Technique	Surface tension σ (10^{-3} N·m^{-1})	Temperature coefficient dσ/dT (10^{-3} N·m^{-1}·K^{-1})	Temperature range T (K)
ESL	1,795 ± 74.3	−0.1790 ± 0.1288	1,900–2,200
EML (CIT)	1,799 ± 20.4	−0.1253 ± 0.0675	1,950–2,600
EML (DLR)	1,804 ± 32.8	−0.1280 ± 0.0857	2,030–2,240
ADL	1,778 ± 36.0	−0.1606 ± 0.0655	2,080–2,830

4 Discussion

The temperature dependence of the density of liquid platinum, which is essential for surface tension measurements, was measured using ESL. The measurement results were in good agreement with those reported by Gathers et al. [31] and Ishikawa et al. [4] (*cf*. Figure 4). Using this result, the surface tension of liquid platinum unaffected by oxygen adsorption was measured by the oscillating droplet method using four different levitation apparatuses: ESL, two EMLs, and ADL. Although the measurements with ESL and two EMLs demonstrated almost identical surface tension temperature dependence, lower values were obtained with ADL. In this section, to support the validity of our measurements, the uncertainties in the measurements are evaluated based on GUM [30].

4.1 Uncertainty for density measurement using ESL

The mass of the levitated droplet, M, that was used for density calculation was determined from the value measured after the solidification. This value is consistent with the mass measured prior to the experiment due to the absence of evaporation during the experiments. The volume of the levitated droplet used in ESL was determined from its 2D image observed from the horizontal direction by the HSV camera. The droplet diameter (d) was converted from pixels (px) to meters (m) by using the reference sphere, the diameter of which (d^{ref}) was measured using a micrometer. Therefore, the main sources of uncertainty in the density measurement using ESL were the calibration of the electronic balance (m_{cal}), measurement resolution of the balance (m_{res}), repeatability of the sample mass measurements performed using the balance (m_{rep}), calibration of the micrometer ($d_{\mathrm{cal}}^{\mathrm{ref}}$), measurement resolution of the micrometer ($d_{\mathrm{res}}^{\mathrm{ref}}$), repeatability of the diameter measurements for the reference sphere using the micrometer ($d_{\mathrm{rep}}^{\mathrm{ref}}$), resolutions of the HSV camera images for the levitated droplet (dp_{res}) and the reference sphere ($dp_{\mathrm{res}}^{\mathrm{ref}}$), repeatability of the numerical contour fittings for the levitated droplet (dp_{rep}) and the reference sphere ($dp_{\mathrm{rep}}^{\mathrm{ref}}$), and droplet volume conversions from the 2D images (V_{rep}). The combined standard uncertainty in the density measurement [$u_{\mathrm{c}}(\rho)$] can be evaluated using the uncertainty contributions [$u_\rho(i)$] of each source (i), as follows:

$$u_c(\rho) = \sqrt{\begin{aligned}&[u_\rho(m_{\mathrm{cal}})]^2 + [u_\rho(m_{\mathrm{res}})]^2 + [u_\rho(m_{\mathrm{rep}})]^2 \\ &\quad + [u_\rho(dp_{\mathrm{res}}^{\mathrm{ref}})]^2 \\ &+[u_\rho(d_{\mathrm{cal}}^{\mathrm{ref}})]^2 + [u_\rho(d_{\mathrm{rep}}^{\mathrm{ref}})]^2 + [u_\rho(dp_{\mathrm{res}}^{\mathrm{ref}})]^2 \\ &\quad + [u_\rho(dp_{\mathrm{rep}}^{\mathrm{ref}})]^2 \\ &+[u_\rho(rp_{\mathrm{res}})]^2 + [u_\rho(rp_{\mathrm{rep}})]^2 + [u_\rho(V_{\mathrm{rep}})]^2\end{aligned}}, \quad (13)$$

where $u_\rho(i)$ is obtained by multiplying the individual standard uncertainty [$u(i)$] and the sensitivity coefficient [$c(i)$] for each source. As a representative example, Table 4 shows the uncertainty budget for the density measurement of liquid platinum using ESL when the largest value of the combined standard uncertainty is obtained for all plots. The standard uncertainties for the repeatability of the sample mass measurements using the balance [$u(m_{\mathrm{rep}})$] and the diameter measurements for the reference sphere using the micrometer [$u(d_{\mathrm{rep}}^{\mathrm{ref}})$] were evaluated based on 10 repeated measurements for the same sample. $u(V_{\mathrm{rep}})$ was calculated as the estimated standard deviation of the volume of the reference sphere estimated from the reference sphere image a few dozen times. When the coverage factor $k_{\mathrm{p}} = 2$ is selected to expand the uncertainty in our measurement plots to satisfy 95.45% confidence, the maximum value was calculated as ±710 kg·m^{-3}, corresponding to approximately ±3.78% for the measurement plots. This indicates that the uncertainty of our density measurement is sufficiently low.

4.2 Uncertainty for surface tension measurement by ESL

As described in equations (2)–(6), the oscillating droplet method employing ESL enables the calculation of the surface tension of a levitated droplet based on seven parameters: r, ρ, M, $f_{2,0}$, F, U, and L. The sources of uncertainty in the surface tension measurement performed using ESL with respect to r and M are $d_{\mathrm{cal}}^{\mathrm{ref}}$, $d_{\mathrm{res}}^{\mathrm{ref}}$, $d_{\mathrm{rep}}^{\mathrm{ref}}$, $dp_{\mathrm{rep}}^{\mathrm{ref}}$, rp_{rep}, $dp_{\mathrm{rep}}^{\mathrm{ref}}$, dp_{res}, m_{cal}, m_{res}, and m_{rep}, same as in the case of the density measurement. For $f_{2,0}$, U, and L, the uncertainties that must be considered include the frequency resolution of the FFT analysis (f_{res}), repeatability of the FFT frequency analysis (f_{rep}), resolution of the measured electrode potential (U_{res}), stability of the electrode potential (U_{sta}), scale resolution for measuring the distance between the electrodes (L_{res}), and repeatability of these distance measurements (L_{rep}). Therefore, the combined standard uncertainty in the surface tension measurement $u_{\mathrm{c}}(\sigma_{\mathrm{ESL}})$ can be evaluated as follows:

Table 4: Uncertainty budget of density measurements of liquid platinum using ESL for the largest calculated uncertainty

Source of uncertainty	Value	Divisor	Standard uncertainty $u(i)$	Sensitivity coefficient $c(i)$	Uncertainty contribution $u_\rho(i)$
Resolution of electro balance	5×10^{-7} kg	$\sqrt{3}$	2.89×10^{-7} kg	4.77×10^{8} m^{-3}	138 kg·m^{-3}
Calibration uncertainty of electro balance	2×10^{-7} kg	2	1×10^{-7} kg	4.77×10^{8} m^{-3}	47.7 kg·m^{-3}
Repeatability of mass measurement	4.22×10^{-7} kg	1	4.22×10^{-7} kg	4.77×10^{8} m^{-3}	201 kg·m^{-3}
Calibration uncertainty of micrometer	2×10^{-6} m	2	1×10^{-6} m	-2.96×10^{7} kg·m^{-4}	−29.6 kg·m^{-3}
Resolution of micrometer	5×10^{-6} m	$\sqrt{3}$	2.89×10^{-6} m	-2.96×10^{7} kg·m^{-4}	−85.3 kg·m^{-3}
Repeatability of diameter measurement	3.68×10^{-6} m	1	3.68×10^{-6} m	-2.96×10^{7} kg·m^{-4}	−109 kg·m^{-3}
Resolution of HSV image for reference sphere	0.5 px	$\sqrt{3}$	0.289 px	190 kg·m^{-3}·px^{-1}	55 kg·m^{-3}
Repeatability of contour fitting on HSV image of reference sphere	0.613 Hz	1	0.613 Hz	190 kg·m^{-3}·Hz^{-1}	117 kg·m^{-3}
Resolution of HSV image for droplet	0.5 px	$\sqrt{3}$	0.289 px	−240 kg·m^{-3}·px^{-1}	−69.2 kg·m^{-3}
Repeatability of contour fitting on HSV image of droplet	0.613 Hz	1	0.613 Hz	−240 kg·m^{-3}·Hz^{-1}	−147 kg·m^{-3}
Volume converted from HSV image of droplet	4.24×10^{-12} m^3	1	4.24×10^{-12} m^3	-8.99×10^{12} kg·m^{-6}	−37.9 kg·m^{-3}
Combined uncertainty, $u_c(\rho)$ = 355 kg·m^{-3}					
Expanded uncertainty, u_{exp} = 710 × 10^{-3} kg·m^{-3} (coverage factor k_p = 2)					

$$u_c(\sigma_{ESL}) = \sqrt{\begin{aligned}&[u_\sigma(d_{cal}^{ref})]^2 + [u_\sigma(d_{res}^{ref})]^2 + [u_\sigma(d_{rep}^{ref})]^2 \\ &+ [u_\sigma(dp_{res}^{ref})]^2 + [u_\sigma(dp_{rep}^{ref})]^2 \\ &+ [u_\sigma(rp_{res})]^2 + [u_\sigma(rp_{rep})]^2 \\ &+ [u_\sigma(m_{cal})]^2 + [u_\sigma(m_{res})]^2 \\ &+ [u_\sigma(m_{rep})]^2 + [u_\sigma(f_{2,0_{rep}})]^2 \\ &+ [u_\sigma(f_{2,0_{rep}})]^2 + [u_\sigma(F)]^2 + [u_\sigma(\rho)]^2 \\ &+ [u_\sigma(L_{res})]^2 + [u_\sigma(L_{rep})]^2 + [u_\sigma(U_{res})]^2 \\ &+ [u_\sigma(U_{sta})]^2.\end{aligned}} \quad (14)$$

Table 5 presents the uncertainty budget for the surface tension measurement of liquid platinum using ESL when the calculated result of the uncertainty for the measurement plot showed the largest value. $u(f_{2,0_{rep}})$ was determined based on a sampling rate of 4,096 Hz when monitoring the surface oscillation for 1 s. $u(f_{2,0_{rep}})$ was evaluated based on four repeated identifications of the surface oscillations, using different samples with the same mass and temperature. $u_\sigma(U_{sta})$ was derived from the variations within the indicated values in ±300 V. In this study, with a selected coverage factor $k_p = 2$, the largest uncertainty in the surface tension measurement with ESL was calculated as ±74.3 × 10^{-3} N·m^{-3}. This represents approximately ±4.1% of the measured values. The droplet density makes the largest contribution to this uncertainty.

4.3 Uncertainty for surface tension measurement by EML

In the oscillating droplet method employed using EML, the surface tension of a levitated droplet is calculated from seven parameters: M, $f_{2,0}$, $f_{2,\pm1}$, $f_{2,\pm2}$, $f_{1,0}$, $f_{1,\pm1}$, and ρ, as described in equations (9) and (10). The combined standard uncertainty in the surface tension measurement $u_c(\sigma_{EML})$ can be evaluated from the following equation:

$$u_c(\sigma_{EML}) = \sqrt{\begin{aligned}&[u_\sigma(m_{cal})]^2 + [u_\sigma(m_{res})]^2 + [u_\sigma(m_{rep})]^2 \\ &+ [u_\sigma(f_{2,0_{res}})]^2 + [u_\sigma(f_{2,\pm1_{res}})]^2 \\ &+ [u_\sigma(f_{2,\pm2_{res}})]^2 + [u_\sigma(f_{1,0_{res}})]^2 \\ &+ [u_\sigma(f_{1,\pm1_{res}})]^2 + [u_\sigma(f_{2,0_{rep}})]^2 \\ &+ [u_\sigma(f_{2,\pm1_{rep}})]^2 + [u_\sigma(f_{2,\pm2_{rep}})]^2 \\ &+ [u_\sigma(f_{1,0_{rep}})]^2 + [u_\sigma(f_{1,\pm1_{rep}})]^2 \\ &+ [u_\sigma(\rho)]^2.\end{aligned}} \quad (15)$$

Table 5: Uncertainty budget of surface tension measurements of liquid platinum using ESL for the largest calculated uncertainty

Source of uncertainty	Value	Divisor	Standard uncertainty $u(i)$	Sensitivity coefficient $c(i)$	Uncertainty contribution $u_\sigma(i)$
Resolution of micrometer	5×10^{-6} m	$\sqrt{3}$	2.89×10^{-6} m	4.49×10^{-2} N·m^{-2}	1.3×10^{-7} N·m^{-1}
Calibration uncertainty of micrometer	2×10^{-6} m	2	1×10^{-6} m	4.49×10^{-2} N·m^{-2}	4.49×10^{-8} N·m^{-1}
Repeatability of diameter measurement	3.68×10^{-6} m	1	3.68×10^{-6} m	4.49×10^{-2} N·m^{-2}	1.65×10^{-7} N·m^{-1}
Resolution of HSV image for reference sphere	0.5 px	$\sqrt{3}$	0.289 px	-1.77×10^{-2} N·m^{-1}·px^{-1}	5.1×10^{-3} N·m^{-1}
Repeatability of contour fitting on HSV image of reference sphere	0.613 Hz	1	0.613 px	-1.77×10^{-2} N·m^{-1}·px^{-1}	1.08×10^{-2} N·m^{-1}
Resolution of HSV image for droplet	0.5 px	$\sqrt{3}$	0.289 px	4.45×10^{-2} N·m^{-1}·px^{-1}	1.28×10^{-2} N·m^{-1}
Repeatability of contour fitting on HSV image of droplet	0.613 px	1	0.613 px	4.45×10^{-2} N·m^{-1}·px^{-1}	2.72×10^{-2} N·m^{-1}
Resolution of electro balance	5×10^{-7} kg	$\sqrt{3}$	2.89×10^{-7} kg	−899 N·m^{-1}·kg^{-1}	-2.7×10^{-5} N·m^{-1}
Calibration uncertainty of electro balance	2×10^{-7} kg	2	1×10^{-7} kg	−899 N·m^{-1}·kg^{-1}	-9×10^{-5} N·m^{-1}
Repeatability of mass measurement	4.22×10^{-7} kg	1	4.22×10^{-7} kg	−899 N·m^{-1}·kg^{-1}	3.79×10^{-4} N·m^{-1}
Resolution of FFT analysis for surface oscillation frequency	0.5 Hz	$\sqrt{3}$	0.289 Hz	1.87×10^{-2} N·m^{-1}·Hz^{-1}	5.4×10^{-3} N·m^{-1}
Repeatability of identification for $f_{2,0}$ via FFT analysis	6.96×10^{-2} Hz	1	0.866 Hz	1.87×10^{-2} N·m^{-1}·Hz^{-1}	1.3×10^{-3} N·m^{-1}
Uncertainty of density measurement	351 kg·m^{-3}	1	351 kg·m^{-3}	9.66×10^{-5} N kg·m^{2}	3.4×10^{-2} N·m^{-1}
Resolution of electron potential control	50 V	$\sqrt{3}$	28.9 V	2.09×10^{-9} N·m^{-1}·V^{-1}	6.04×10^{-5} N·m^{-1}
Repeatability of electron potential control	300 V	1	300 V	2.09×10^{-9} N·m^{-1}·V^{-1}	6.28×10^{-4} N·m^{-1}
Resolution of scale	0.25×10^{-3} m	$\sqrt{3}$	1.44×10^{-3} m	3.64 N·m^{-2}	5.26×10^{-4} N·m^{-1}
Repeatability of electrode distance measurements	0.5×10^{-3} m	1	0.5×10^{-3} m	3.64 N·m^{-2}	1.05×10^{-3} N·m^{-1}
Uncertainty of correction term F	6.77×10^{-4}	1	6.77×10^{-4}	1.8 N·m^{-1}	1.21×10^{-3} N·m^{-1}
Combined uncertainty, $u_c(\sigma_{ESL}) = 37.1 \times 10^{-3}$ N·m^{-1}					
Expanded uncertainty, $u_{exp} = 74.3 \times 10^{-3}$ N·m^{-1} (coverage factor $k_p = 2$)					

Table 6: Uncertainty budget of surface tension measurements of liquid platinum using EML installed at CIT for the largest calculated uncertainty

Source of uncertainty	Value	Divisor	Standard uncertainty $u(i)$	Sensitivity coefficient $c(i)$	Uncertainty contribution $u_\sigma(i)$
Calibration of electronic balances	1×10^{-8} kg	2	5×10^{-9} kg	685 $N \cdot m^{-1} \cdot kg^{-1}$	1.97×10^{-5} $N \cdot m^{-1}$
Measuring resolution of electronic balance	5×10^{-8} kg	$\sqrt{3}$	2.89×10^{-8} kg	685 $N \cdot m^{-1} \cdot kg^{-1}$	3.42×10^{-6} $N \cdot m^{-1}$
Repeatability of sample mass measurement	4.22×10^{-7} kg	1	4.22×10^{-7} kg	685 $N \cdot m^{-1} \cdot kg^{-1}$	2.89×10^{-5} $N \cdot m^{-1}$
Frequency resolution of FFT analysis for $m = 0$ in $l = 1$	3.05×10^{-2} Hz	$\sqrt{3}$	1.76×10^{-2} Hz	5.09×10^{-2} $N \cdot m^{-1} \cdot Hz^{-1}$	8.96×10^{-3} $N \cdot m^{-1}$
Repeatability of identification for $f_{1,0}$ via FFT analysis	2.66×10^{-2} Hz	1	2.66×10^{-2} Hz	5.09×10^{-2} $N \cdot m^{-1} \cdot Hz^{-1}$	1.35×10^{-3} $N \cdot m^{-1}$
Frequency resolution of FFT analysis for $m = -1$ in $l = 1$	3.05×10^{-2} Hz	$\sqrt{3}$	1.76×10^{-2} Hz	4.76×10^{-2} $N \cdot m^{-1} \cdot Hz^{-1}$	8.39×10^{-4} $N \cdot m^{-1}$
Repeatability of identification for $f_{1,-1}$ via FFT analysis	7.63×10^{-2}·Hz	1	3.9×10^{-2} Hz	4.76×10^{-2} $N \cdot m^{-1} \cdot Hz^{-1}$	1.86×10^{-3} $N \cdot m^{-1}$
Frequency resolution of FFT analysis for $m = +1$ in $l = 1$	3.05×10^{-2} Hz	$\sqrt{3}$	1.76×10^{-2} Hz	8.66×10^{-2} $N \cdot m^{-1} \cdot Hz^{-1}$	1.53×10^{-3} $N \cdot m^{-1}$
Repeatability of identification for $f_{1,+1}$ via FFT analysis	7.63×10^{-2} Hz	1	7.63×10^{-2} Hz	8.66×10^{-2} $N \cdot m^{-1} \cdot Hz^{-1}$	6.6×10^{-3} $N \cdot m^{-1}$
Frequency resolution of FFT analysis for $m = 0$ in $l = 2$	3.05×10^{-2} Hz	$\sqrt{3}$	1.76×10^{-2} Hz	2.98×10^{-2} $N \cdot m^{-1} \cdot Hz^{-1}$	5.25×10^{-4} $N \cdot m^{-1}$
Repeatability of identification for $f_{2,0}$ via FFT analysis	1.73×10^{-2} Hz	1	1.73×10^{-2} Hz	2.98×10^{-2} $N \cdot m^{-1} \cdot Hz^{-1}$	5.15×10^{-4} $N \cdot m^{-1}$
Frequency resolution of FFT analysis for $m = \pm 1$ in $l = 2$	3.05×10^{-2} Hz	$\sqrt{3}$	1.76×10^{-2} Hz	7.57×10^{-2} $N \cdot m^{-1} \cdot Hz^{-1}$	1.33×10^{-3} $N \cdot m^{-1}$
Repeatability of identification for $f_{2,\pm 1}$ via FFT analysis	1.47×10^{-2} Hz	1	1.47×10^{-2} Hz	7.57×10^{-2} $N \cdot m^{-1} \cdot Hz^{-1}$	1.11×10^{-2} $N \cdot m^{-1}$
Frequency resolution of FFT analysis for $m = \pm 2$ in $l = 2$	3.05×10^{-2} Hz	$\sqrt{3}$	1.76×10^{-2} Hz	7.57×10^{-2} $N \cdot m^{-1} \cdot Hz^{-1}$	1.33×10^{-3} $N \cdot m^{-1}$
Repeatability of identification for $f_{2,\pm 2}$ via FFT analysis	1.03×10^{-2} Hz	1	1.03×10^{-2} Hz	7.57×10^{-2} $N \cdot m^{-1} \cdot Hz^{-1}$	7.8×10^{-3} $N \cdot m^{-1}$
Reported density for liquid platinum	343 $kg \cdot m^{-3}$	1	343 $kg \cdot m^{-3}$	-1.58×10^{-5} $Nm^2 \cdot kg^{-1}$	-5.4×10^{-3} $N \cdot m^{-1}$
Combined uncertainty, $u_c(\sigma_{EML})$: 16.4×10^{-3} $N \cdot m^{-1}$					
Expanded uncertainty, u_{exp}: 32.8×10^{-3} $N \cdot m^{-1}$ (coverage factor $k_p = 2$)					

Table 7: Uncertainty budget of surface tension measurements of liquid platinum using EML installed at DLR for the largest calculated uncertainty

Source of uncertainty	Value	Divisor	Standard $u(i)$	Sensitivity coefficient $c(i)$	Uncertainty contribution $u_\sigma(i)$
Calibration of electronic balances	1×10^{-8} kg	2	5×10^{-9} kg	1.17×10^{3} N·m^{-1}·kg^{-1}	3.39×10^{-7} N·m^{-1}
Measuring resolution of electronic balance	5×10^{-10} kg	$\sqrt{3}$	2.89×10^{-10} kg	1.17×10^{3} N·m^{-1}·kg^{-1}	5.87×10^{-6} N·m^{-1}
Repeatability of sample mass measurement	4×10^{-9} kg	2	2×10^{-9} kg	1.17×10^{3} N·m^{-1}·kg^{-1}	2.35×10^{-6} N·m^{-1}
Frequency resolution of FFT analysis for $m = 0$ in $l = 1$	7.75×10^{-2} Hz	$\sqrt{3}$	4.48×10^{-2} Hz	1.94×10^{-2} N·m^{-1}·Hz^{-1}	8.68×10^{-4} N·m^{-1}
Repeatability of identification for $f_{1,0}$ via FFT analysis	1.59×10^{-1} Hz	1	1.59×10^{-1} Hz	1.94×10^{-2} N·m^{-1}·Hz^{-1}	3.08×10^{-3} N·m^{-1}
Frequency resolution of FFT analysis for $m = -1$ in $l = 1$	7.75×10^{-2} Hz	$\sqrt{3}$	4.48×10^{-2} Hz	1.18×10^{-2} N·m^{-1}·Hz^{-1}	5.26×10^{-4} N·m^{-1}
Repeatability of identification for $f_{1,-1}$ via FFT analysis	4.71×10^{-4} Hz	1	4.71×10^{-4} Hz	1.18×10^{-2} N·m^{-1}·Hz^{-1}	5.54×10^{-6} N·m^{-1}
Frequency resolution of FFT analysis for $m = +1$ in $l = 1$	7.75×10^{-2} Hz	$\sqrt{3}$	4.48×10^{-2} Hz	1.18×10^{-2} N·m^{-1}·Hz^{-1}	5.26×10^{-4} N·m^{-1}
Repeatability of identification for $f_{1,+1}$ via FFT analysis	9.24×10^{-2} Hz	1	9.24×10^{-2} Hz	1.18×10^{-2} N·m^{-1}·Hz^{-1}	1.09×10^{-3} N·m^{-1}
Frequency resolution of FFT analysis for $m = 0$ in $l = 2$	7.75×10^{-2} Hz	$\sqrt{3}$	4.48×10^{-2} Hz	2.43×10^{-2} N·m^{-1}·Hz^{-1}	1.09×10^{-4} N·m^{-1}
Repeatability of identification for $f_{2,0}$ via FFT analysis	2.73×10^{-1} Hz	1	2.73×10^{-1} Hz	2.43×10^{-2} N·m^{-1}·Hz^{-1}	6.64×10^{-3} N·m^{-1}
Frequency resolution of FFT analysis for $m = \pm 1$ in $l = 2$	7.75×10^{-2} Hz	$\sqrt{3}$	4.48×10^{-2} Hz	5.29×10^{-2} N·m^{-1}·Hz^{-1}	2.37×10^{-4} N·m^{-1}
Repeatability of identification for $f_{2,\pm 1}$ via FFT analysis	9.24×10^{-2} Hz	1	9.24×10^{-2} Hz	5.29×10^{-2} N·m^{-1}·Hz^{-1}	4.89×10^{-3} N·m^{-1}
Frequency resolution of FFT analysis for $m = \pm 2$ in $l = 2$	7.75×10^{-2} Hz	$\sqrt{3}$	4.48×10^{-2} Hz	5.14×10^{-2} N·m^{-1}·Hz^{-1}	2.3×10^{-4} N·m^{-1}
Repeatability of identification for $f_{2,\pm 2}$ via FFT analysis	4.6×10^{-2} Hz	1	4.6×10^{-2} Hz	5.14×10^{-2} N·m^{-1}·Hz^{-1}	2.36×10^{-3} N·m^{-1}
Reported density for liquid platinum	350 kg·m^{-3}	1	350 kg·m^{-3}	-6.99×10^{-6} N·m^{2}·kg^{-1}	-2.45×10^{-3} N·m^{-1}
Combined uncertainty, $u_c(\sigma_{EML})$: 10.2×10^{-3} N·m^{-1}					
Expanded uncertainty, u_{exp}: 20.4×10^{-3} N·m^{-1} (coverage factor $k_p = 2$)					

Table 8: Uncertainty budget of surface tension measurements of liquid platinum using ADL for the largest calculated uncertainty

Source of uncertainty	Value	Divisor	Standard uncertainty, $u(i)$	Sensitivity coefficient, $c(i)$	Uncertainty contribution, $u_\sigma(i)$
Calibration of electronic balances	2×10^{-7} kg	2	1×10^{-7} kg	4.49×10^{3} N·m^{-1} kg^{-1}	1.3×10^{-3} N·m^{-1}
Measuring resolution of electronic balance	5×10^{-7} kg	$\sqrt{3}$	2.89×10^{-8} kg	4.49×10^{3} N·m^{-1} kg^{-1}	4.49×10^{-3} N·m^{-1}
Repeatability of sample mass measurement	4.22×10^{-8} kg	1	4.22×10^{-8} kg	4.49×10^{3} N·m^{-1} kg^{-1}	1.9×10^{-3} N·m^{-1}
Resolution of FFT analysis for surface oscillation frequency	1.18 × 10^{-3} Hz	1	1.18×10^{-3} Hz	1.8×10^{-2} N·m^{-1} Hz^{-1}	2.12×10^{-5} N·m^{-1}
Repeatability of identification for $f_{2,0}$ via FFT analysis	1.67 Hz	$\sqrt{3}$	9.62×10^{-1} Hz	1.8×10^{-2} N·m^{-1} Hz^{-1}	1.73×10^{-2} N·m^{-1}
Combined uncertainty, $u_c(\sigma_{ADL}) = 18.0 \times 10^{-3}$ N·m^{-1}					
Expanded uncertainty, $u_{exp} = 36.0 \times 10^{-3}$ N·m^{-1} (coverage factor $k_p = 2$)					

Tables 6 and 7 show the uncertainty budgets in the surface tension measurements of liquid platinum using EMLs installed at CIT and DLR, respectively, when the calculated results of the uncertainties for the measurement plot show the largest values. $u(f_{2,m_{res}})$ and $u(f_{1,m_{res}})$ were determined from five repeated identifications of the surface oscillations for a single sample. When the coverage factor k_p = 2 was selected, the largest values of uncertainties in the surface tension measurement using EML were ±32.8 × 10^{-3} and ±20.4 × 10^{-3} N·m^{-1} for CIT and DLR, respectively. The measurement using the EML of CIT has a slightly larger uncertainty, which can be attributed to the larger sample size.

4.4 Uncertainty for surface tension measurement by ADL

In the determination of the surface tension of an aerodynamically levitated droplet from the Rayleigh equation and parameters m and $f_{2.0}$ [6], the uncertainty $[u_c(\sigma_{ADL})]$ can be evaluated as follows:

$$u_c(\sigma_{ADL}) = \sqrt{\begin{matrix}[u_\sigma(m_{cal})]^2 + [u_\sigma(m_{res})]^2 + [u_\sigma(m_{rep})]^2 \\ + [u_\sigma(f_{2,0_{rep}})]^2 + [u_\sigma(f_{2,0_{rep}})]^2\end{matrix}}. \quad (16)$$

Table 8 presents the uncertainty budget in the surface tension measurement of liquid platinum using ADL when the calculated uncertainty shows the maximum value. $u(f_{res})$ was determined by recording the droplet images at a rate of 2,000 fps for 0.3 s. $u(m_{rep})$ and $u(f_{2,0_{rep}})$ were calculated from seven repeated measurements. When the coverage factor k_p = 2 was selected, the maximum value of $u_c(\sigma_{ADL})$ was ±36.0 × 10^{-3} N·m^{-1}, corresponding to approximately ±2.0% for the measurement plot. The remarkably high value of $u(f_{2,0_{rep}})$ can be attributed to the small sample size, which results in an extremely short decay time for the surface oscillation.

These uncertainty evaluations demonstrate that for various plots of the measured surface tension at high temperatures using ADL, the temperature dependence of the surface tension is lower than those measured with ESL and EMLs beyond the uncertainty in the measurement.

When a droplet is levitated with ESL and EML, external forces such as gravitational acceleration, electric charge, and electromagnetic force induce droplet deformation, thereby altering the frequencies of surface oscillations. Therefore, the effects of droplet deformation by such forces are calibrated to ensure accurate surface tension measurements with ESL and EML. However, in the measurement with ADL, the effects of droplet deformation due to external

forces such as the gas jet pressure, fluid flow induced by the jet stream, and gravitational acceleration have not been adequately considered. To better understand the discrepancies in the measured surface tension values obtained using ESL, EML, and ADL, a further investigation of how the deformation of the aerodynamically levitated droplet affects the behavior of surface oscillations is required.

4.5 Uncertainty for gradients of density and surface tension relative to temperature

The temperature dependence of density can be expressed in the following form:

$$\rho = \hat{\beta}(T - \bar{T}) + \bar{\rho}, \tag{17}$$

where $\hat{\beta}$ is the temperature coefficient of density, and $\bar{T}$ and $\bar{\rho}$ are the mean values of temperature and density, respectively. The uncertainty in $\hat{\beta}$ of this regression line can be predicted using the following equations:

$$u^2(\hat{\beta}) = \frac{\hat{\delta}_e^2 + u_c^2(\rho_i)}{\sum(T_i - \bar{T})^2}, \tag{18}$$

$$\hat{\delta}_e^2 = \frac{\sum\rho - \hat{\beta}(T_i - \bar{T}) + \bar{\rho}}{n - 2}, \tag{19}$$

where $\hat{\delta}_e$ is the residual variance of the measured data and n is the number of measuring plots. By using this formula, the uncertainty in the gradient of the measured density with respect to temperature (equation (11)) was evaluated to be ±0.3888 $kg{\cdot}m^{-3}{\cdot}K^{-1}$ with a $k_p = 2$. Similarly, the uncertainty in the gradient of the measured surface tension with respect to temperature (equation (12)), determined using ESL and EMLs, was evaluated to be $\pm0.0445 \times 10^{-3}$ $N{\cdot}m^{-1}{\cdot}K^{-1}$.

5 Summary

The surface tension of liquid platinum free of any contaminations from the supporting materials and atmospheric oxygen was measured by the oscillating droplet method using ESL, two EMLs, and ADL. In addition, the density was precisely measured with ESL over a wide temperature range of approximately 500 K, including the undercooling conditions. The temperature dependence of the density for liquid platinum was described by a linear fit of the plotted data given by

$$\rho = 18{,}906 \pm 715 - (1.0852 \pm 0.3888) \times (T - 2{,}041)[kg{\cdot}m^{-3}](1{,}700 - 2{,}200\ K).$$

The round-robin measurement of the surface tension of liquid platinum clarified that a nearly identical surface tension-temperature relationship can be obtained using both ESL and EML. When considering the uncertainty in the measurements with ESL and EML, the temperature dependence of the surface tension was described as follows:

$$\sigma = 1{,}798 \pm 74.3 - (0.12 \pm 0.0445) \times (T - 2{,}041)[10^{-3}\ N{\cdot}m^{-1}](1{,}900 - 2{,}600\ K).$$

The surface tensions measured in the round-robin test with ADL were slightly lower than those measured with ESL and EMLs, particularly at higher temperatures, with the discrepancy exceeding the measurement uncertainty. To understand the origin of this discrepancy in the measurement results, it is necessary to investigate the effect of the deformation of the aerodynamically levitated droplet on the surface oscillation behavior.

Acknowledgments: This study was financially supported by JSPS KAKENHI under Grant P20H02453. This study was supported by Grant-in-Aid for Front Loading Research from the Advisory Committee for Space Utilization Research in ISAS/JAXA.

Funding information: This research was partially funded by the Japan Society for the Promotion of Science (JSPS) KAKENHI under Grant No. P20H02453, and by the Grant-in-Aid for Front Loading Research, which is supported by the Advisory Committee for Space Utilization Research in the Institute of Space and Astronautical Science, Japan Aerospace Exploration Agency (ISAS/JAXA).

Author contributions: Yusaku Seimiya: writing – original draft preparation, investigation; Shuto Tomita: investigation; Tohei Kawaguchi: investigation; Hidekazu Kobatake: investigation, review and editing; Jürgen Brillo: investigation, review and editing; Suguru Shiratori: investigation, image analysis, review and editing; Ken-ichi Sugioka: review and editing; Takehiko Ishikawa: investigation, review and editing; Shumpei Ozawa: supervision, writing – original draft preparation, writing – review and editing, investigation, resource.

Conflict of interest: The authors state no conflict of interest.

Data availability statement: The data that support the findings of this study are available from the corresponding author upon reasonable request.

References

[1] Rhim, W.-K., K. Ohsaka, and P.-F. Paradis. Noncontact technique for measuring surface tension and viscosity of molten materials using high temperature electrostatic levitation. *Review of Scientific Instruments*, Vol. 70, No. 6, 1999, pp. 2796–2801.

[2] Rhim, W.-K. and P.-F. Paradis. Laser-induced rotation of a levitated sample in vacuum. *Review of Scientific Instruments*, Vol. 7012, 1999, pp. 4652–4655.

[3] Ishikawa, T. and P.-F. Paradis. Thermophysical properties of molten refractory metals measured by an electrostatic levitator. *Journal of Electronic Materials*, Vol. 3412, 2005, pp. 1526–1532.

[4] Ishikawa, T., P.-F. Paradis, and N. Koike. Non-contact thermophysical property measurements of liquid and supercooled platinum. *Japanese Journal of Applied Physics*, Vol. 453A, 2006, pp. 1719–1724.

[5] Seimiya, Y., Y. Kudo, R. Shinazawa, Y. Watanabe, T. Ishikawa, and S. Ozawa. Round-robin measurement of surface tension for liquid titanium by Electromagnetic Levitation (EML) and Electrostatic Levitation (ESL). *Metals*, Vol. 12, No. 7, 2022, id. 1129.

[6] Egry, I., E. Ricci, R. Novakovic, and S. Ozawa. Surface tension of liquid metals and alloys – Recent developments. *Advances in Colloid and Interface Science*, Vol. 159, 2010, pp. 198–212.

[7] Lohöfer, G., J. Brillo, and I. Egry. Thermophysical Properties of Undercooled Liquid Cu–Ni Alloys. *International Journal of Thermophysics*, Vol. 25, No. 5, 2004, pp. 1535–1550.

[8] Ozawa., S., K. Morohoshi, T. Hibiya, and H. Fukuyama. Influence of oxygen partial pressure on surface tension of molten silver. *Journal of Applied Physics*, Vol. 107, 2010, id. 014910.

[9] Ozawa, S., S. Takahashi, S. Suzuki, H. Sugawara, and H. Fukuyama. Influence of oxygen partial pressure on surface tension and its temperature coefficient of molten iron. *Journal of Applied Physics*, Vol. 109, 2011, id. 014902.

[10] Ozawa, S., S. Takahashi, N. Watanabe, and H. Fukuyama. Influence of oxygen adsorption on surface tension of molten nickel measured under reducing gas atmosphere. *International Journal of Thermophysics*, Vol. 35, 2014, pp. 1705–1711.

[11] Ozawa, S., M. Nishimura, and K. Kuribayashi. Surface tension of molten silver in consideration of oxygen adsorption measured by electromagnetic levitation. *International Journal of Microgravity Science and Applications*, Vol. 33, No. 3, 2016, id. 330310.

[12] Ozawa, S., Y. Nagasaka, M. Itakura, K. Sugisawa, and Y. Seimiya. Influence of oxygen adsorption from atmosphere on surface tension of liquid silicon. *Journal of Applied Physics*, Vol. 130, 2021, id. 135101.

[13] Brillo, J. and I. Egry. Surface tension of nickel, copper, iron and their binary alloys. *Journal of Materials Science*, Vol. 40, 2005, pp. 2213–2216.

[14] Brillo, J., J. Wessing, H. Kobatake, and H. Fukuyama. Surface tension of liquid Ti with adsorbed oxygen and its prediction. *Journal of Molecular Liquids*, Vol. 290, No. 15, 2019, id. 111226.

[15] Glorieux, B., F. Millot, and J. C. Rifflet. Surface tension of liquid alumina from contactless techniques. *International Journal of Thermophysics*, Vol. 23, No. 5, 2002, pp. 1249–1257.

[16] Hakamada, S., A. Nakamura, M. Watanabe, and F. Kargl. Surface oscillation phenomena of aerodynamically levitated Molten Al_2O_3. *International Journal of Microgravity Science and Application*, Vol. 34, No. 4, 2017, id. 340403.

[17] Kargl, F., C. Yuan, and G. Greaves. Aerodynamic Levitation: Thermophysical property measurements of liquid oxides. *International Journal of Microgravity Science and Application*, Vol. 32, No. 2, 2015, id. 320212.

[18] Maux, D., V. Klapczynski, M. Courtois, T. Pierre, and P. Masson. Surface tension of liquid Fe, Nb and 304L SS and effect of drop mass in aerodynamic levitation. *Journal of Materials Science*, Vol. 57, 2022, pp. 12094–12106.

[19] Rayleigh, L. On the capillary phenomena of jets. *Proceedings of the Royal Society of London*, Vol. 29, 1879, pp. 71–97.

[20] Egry, I., H. Giffard, and S. Schneider. The oscillating drop technique revisited. *Measurement Science and Technology*, Vol. 16, No. 2, 2005, pp. 426–431.

[21] Higuchi, K., M. Watanabe, R. K. Wunderlich, and H.-J. Fecht. Analysis of surface tension and viscosity by oscillation drop method including sample rotation effects. *International Journal of Microgravity Science and Application*, Vol. 24, 2007, pp. 169–175.

[22] Ozawa, S., T. Koda, M. Adachi, S. Shiratori, N. Takenaga, T. Hibiya, et al. Identifying rotation and oscillation in surface tension measurement using an oscillating droplet method. *Heat Transfer – Asian Research*, Vol. 37, No. 7, 2008, pp. 421–430.

[23] Ozawa, S., T. Koda, M. Adachi, K. Morohoshi, M. Watanabe, and T. Hibiya. The influence of temporal phase difference of $m = \pm 2$ oscillations on surface tension frequency analysis for levitated droplets. *Journal of Applied Physics*, Vol. 106, 2009, id. 034907.

[24] Ozawa, S., Y. Kudo, K. Kuribayashi, Y. Watanabe, and T. Ishikawa. Precise density measurement of liquid titanium by electrostatic levitator. *Materials Transaction*, Vol. 5812, 2017, pp. 1664–1669.

[25] Rayleigh, L. On the equilibrium of liquid conducting masses charged with electricity. *Philosophical Magazine*, Vol. 14, No. 87, 1882, pp. 184–186.

[26] Feng, J. Q. and K. V. Beard. Small-amplitude oscillations of electrostatically levitated drops. *Proceedings of the Royal Society of London*, Vol. A430, 1990, pp. 133–150.

[27] Cummings, D. L. and D. A. Blackburn. Oscillations of magnetically levitated aspherical droplets. *Journal of Fluid Mechanics*, Vol. 224, 1991, pp. 395–416.

[28] Aoyama, T., Y. Takamura, and K. Kuribayashi. Conteinerless solidification of Si-Ge binary alloy by means of laser heating electromagnetic levitation. *Japanese Journal of Applied Physics*, Vol. 37, No. 6A, Part 2, 1998, pp. L687–L690.

[29] Dubinin, E. L., V. M. Vlasov, A. I. Timofeev, S. O. Safonov, and A. I. Chegodaev. Temperature dependence of the surface tension and density of molten Pt and Rh, Izvestiya Vysshikh Uchebnykh Zavedenij. *Tsvetnaya Metallurgiya*, Vol. 4, 1975, pp. 160–161.

[30] Hixson, R. S. and M. A. Winkler. Thermophysical properties of liquid platinum. *International Journal of Thermophysics*, Vol. 14, No. 3, 1993, pp. 409–416.

[31] Gathers, G. R., J. W. Shaner, and W. M. Hodgson. *Proceedings of the 6th European Thermophysical Properties Conference*, Dubrovnik, Yugoslavia, June 26–30, 1978.

[32] Eremenko, V. N. and Y. V. Naidich. Measurement of the surface tension and density of liquid platinum. *Izvestiya Akademii Nauk SSSR Otdelenie Tekhnicheskikh Nauk Metallurgiya i Toplivo*, Vol. 6, 1959, pp. 129–131.

[33] Martsenyuk, P. S., Yu. N. Ivashchenko, and V. N. Eremenko. Specific free surface energy of liquid palladium, iridium and platinum at the melting temperature. *Phase Interfaces and Their Properties. Institute of Problems of Materials Sciences*, The National Academy of Sciences of Ukraine, Kiev, 1980.

[34] Nawer, J., T. Ishikawa, H. Oda, C. Koyama, and D. M. Matson. Uncertainty quantification of thermophysical property measurement in space and on earth: A Study of liquid platinum using

electrostatic levitation. *Journal of Astronomy and Space Science*, Vol. 40, No. 3, 2023, pp. 93–100.
[35] Allen, B. C. The Surface tension of liquid transition metals at their melting points. *Transactions of the Metallurgical Society of AIME*, Vol. 227, 1963, pp. 1175–1183.
[36] Vinet, B., J.-P. Garandet, B. Marie, L. Domergue, and B. Drevet. Surface tension measurements on industrial alloys by the drop-weight method. *International Journal of Thermophysics*, Vol. 25, No. 3, 2004, pp. 869–883.
[37] *Guide to the Expression of Uncertainty in Measurement*, ISO, Geneva, 1995.